250 (1:10 dilution; rat IgG2a; Sera-Lab). Secondary antibodies to mouse IgG1 and IgG2b or rat IgG were conjugated to fluorescein isothiocyanate (FITC) or tetramethyl rhodamine isothiocyanate and used at 1:100 dilution in 3% BSA in phosphate-buffered saline (Southern Biotechnology Associates). When BrdU mAb was used, the sections were treated for 15 min in 4 M HCl before the blocking step. Images were captured digitally on a BioRad confocal microscope.
14. T. A. Rando and H. M. Blau, *J. Cell Biol.* **125**, 1275 (1994). A nylon mesh was not used.
15. C. D. Surh and J. Sprent, *Nature* **372**, 100 (1994).
16. H. S. R. Coles *et al.*, *Development* **118**, 777 (1993).
17. We thank X. Yu for her work on apoptosis, S. Fraser and K. Woo for imaging and lineage tracing assistance, W. Wright for myogenin mAb cell line F5D, N. Shah for antibodies, J. Miano and E. Olson for SM-MHC plasmid, C. Cardell for technical assistance, and D. Anderson, P. Garrity, N. Hong, J. Miner, P. Mueller, P. Patterson, and members of Wold group for comments. Supported by NIH grant AR40708 to B.W. A.P. was supported by an NIH Predoctoral Training Grant.

10 July 1995; accepted 6 November 1995

Crystal Structure of the V_α Domain of a T Cell Antigen Receptor

Barry A. Fields, Bertram Ober, Emilio L. Malchiodi, Marina I. Lebedeva, Bradford C. Braden, Xavier Ysern, Jin-Kyoo Kim, Xuguang Shao, E. Sally Ward, Roy A. Mariuzza*

The crystal structure of the V_α domain of a T cell antigen receptor (TCR) was determined at a resolution of 2.2 angstroms. This structure represents an immunoglobulin topology set different from those previously described. A switch in a polypeptide strand from one β sheet to the other enables a pair of V_α homodimers to pack together to form a tetramer, such that the homodimers are parallel to each other and all hypervariable loops face in one direction. On the basis of the observed mode of V_α association, a model of an $(\alpha\beta)_2$ TCR tetramer can be positioned relative to the major histocompatibility complex class II $(\alpha\beta)_2$ tetramer with the third hypervariable loop of V_α over the amino-terminal portion of the antigenic peptide and the corresponding loop of V_β over its carboxyl-terminal residues. TCR dimerization that is mediated by the α chain may contribute to the coupling of antigen recognition to signal transduction during T cell activation.

T lymphocytes recognize a wide variety of antigens through highly diverse cell-surface glycoproteins known as TCRs. These molecules are composed of α and β (or γ and δ) chains that have variable (V) and constant (C) regions homologous to those of antibodies (*1*). However, antibodies recognize antigen in intact form, whereas TCRs recognize antigen only as peptide fragments bound to molecules of the major histocompatibility complex (MHC) (*2*). The three-dimensional structure of the extracellular portion of the β chain of a murine TCR (V_α4.1-J_α2B4, V_β8.2-J_β2.1) specific for a hemagglutinin peptide of influenza virus (HA-110–120) in the context of the MHC class II I-E^d molecule has been solved (*3*). A TCR designated 1934.4, which is specific for the NH_2-terminal nonapeptide of myelin basic protein (Ac1–9) in association with I-A^u (*4*), is encoded by the closely related V_α4.2-J_α4.0, V_β8.2-J_β2.3 gene combination (*5*). Injection into mice of the T cell clone from which the 1934.4 TCR was isolated induces experimental autoimmune encephalomyelitis, a model for human multiple sclerosis (*6*). The V_α domain of this pathogenic TCR has been produced and crystallized (*7*, *8*); here, we describe its crystal structure at 2.2 Å resolution (*9*).

The V_α domain exists as a homodimer both in solution (*8*) and in the crystal structure (Fig. 1A). The relative orientation of the two chains in the homodimer is almost identical to that in antibody V_LV_H dimers, with peptide loops homologous to the complementarity-determining regions (CDRs) of antibodies disposed to form part of the antigen-binding site. Fourteen residues from each V_α domain contribute numerous van der Waals contacts and 10 hydrogen bonds across the homodimer interface. Of these, residues Tyr^{35}, Gln^{37}, Pro^{43}, Tyr^{87}, and Phe^{106} [numbered as in (*10*)] are equivalent by homology to those involved in V_LV_H association (*11*, *12*). These residues are also highly conserved in V_β regions (excluding Pro^{43}, which is most commonly substituted by Leu), which indicates that the geometry of TCR

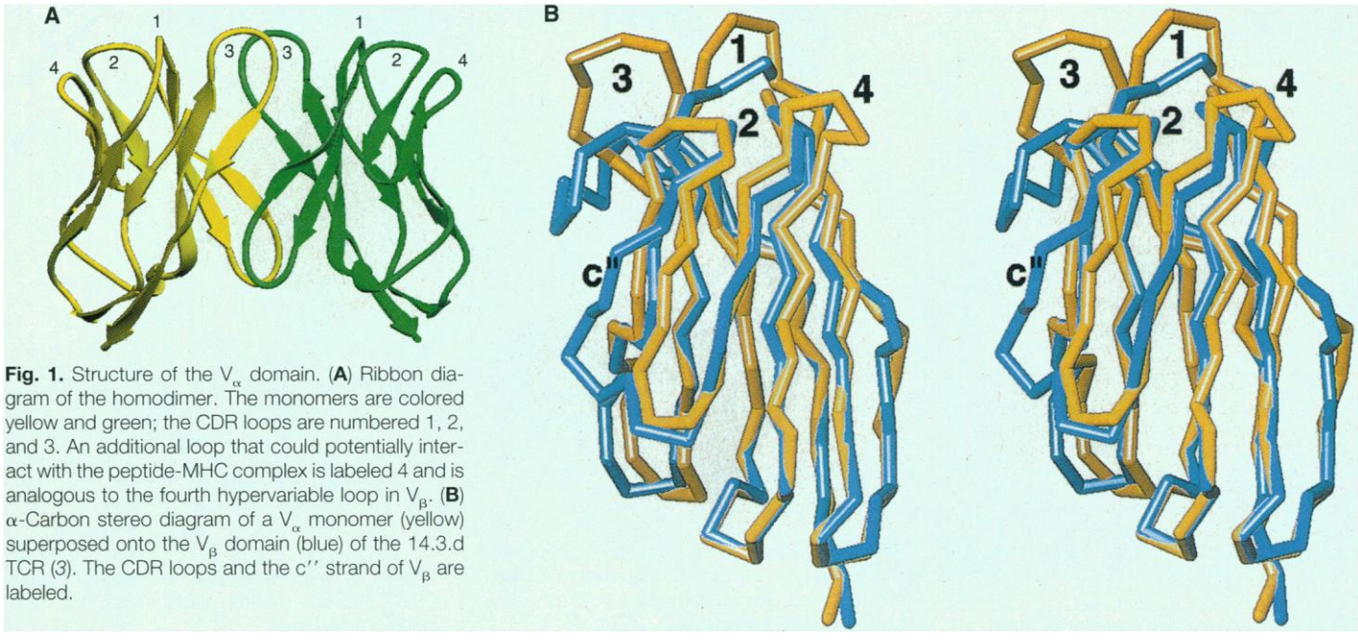

Fig. 1. Structure of the V_α domain. (**A**) Ribbon diagram of the homodimer. The monomers are colored yellow and green; the CDR loops are numbered 1, 2, and 3. An additional loop that could potentially interact with the peptide-MHC complex is labeled 4 and is analogous to the fourth hypervariable loop in V_β. (**B**) α-Carbon stereo diagram of a V_α monomer (yellow) superposed onto the V_β domain (blue) of the 14.3.d TCR (*3*). The CDR loops and the c′′ strand of V_β are labeled.

$V_\alpha V_\beta$ association is likely to be similar to that of $V_L V_H$.

The structural framework of the V_α domain shows significant similarities to immunoglobulin (Ig) V domains [root-mean-square deviations (RMSDs) from superposition onto nine V_L and nine V_H domains are 1.3 and 1.7 Å, respectively] and to V_β (RMSD, 1.2 Å) (Fig. 1B). However, a switch in a polypeptide strand from one β sheet to the other (Fig. 2) distinguishes the β strand topology of V_α from that of other members of the Ig superfamily (*11*, *13*). In antibody V domains, as well as in TCR V_β (*3*), the c′′ strand is hydrogen-bonded to the c′ strand in the same β sheet. In V_α, the c′′ strand is associated with the d strand of the adjacent sheet through six backbone-backbone hydrogen bonds (Fig. 3). The previously defined Ig topology sets have been classified as V (variable; for example, Ig V domains, CD4 domains 1 and 3), C (constant; for example, Ig constant domains), S (switched; for example, CD4 domains 2 and 4), H (hybrid; for example, the cellulase NH_2-terminal domain), and I (intermediate; for example, telokin) (*11*, *13*). We propose that the Ig topology set corresponding to the V_α domain be designated the A set.

The conformation of CDR1 of V_α4.2 appears to be stabilized predominantly by hydrophobic interactions, not by intraloop hydrogen bonding as was observed for V_β8.2 (*3*); however, Tyr^{65}, like Arg^{69} of the known V_β structure, forms a hydrogen bond to the backbone of CDR1 (Fig. 4A). Residues Tyr^{24} and Leu^{32}, which are highly conserved in mouse and human α chain sequences (*10*), pack against each other in the loop. The most common substitution at both positions is Phe, which should preserve or enhance the hydrophobic packing interactions. Residues Ala^{26} and Pro^{30} also contribute to the hydrophobic stabilization, although these positions are more variable. In contrast, CDR1 of both the V_L and V_H domains is mainly stabilized by the hydrophobic side chain of residue 29, which intercalates between two β-pleated sheets. The CDR1 loops in V_α sequences vary in length by up to three amino acids; the 11-residue loop of V_α4.2 is the most frequently observed length (*10*). Together with the conservation of hydrophobic residues at positions 24 and 32, this suggests that the CDR1 conformation described here may be common to many other α chains.

B. A. Fields, E. L. Malchiodi, M. I. Lebedeva, B. C. Braden, R. A. Mariuzza, Center for Advanced Research in Biotechnology, University of Maryland Biotechnology Institute, 9600 Gudelsky Drive, Rockville, MD 20850, USA. B. Ober, J.-K. Kim, X. Shao, E. S. Ward, Cancer Immunobiology Center and Department of Microbiology, University of Texas Southwestern Medical Center, 5323 Harry Hines Boulevard, Dallas, TX 75235–8576, USA. X. Ysern, Center for Drug Evaluation and Research, U.S. Food and Drug Administration, 5600 Fishers Lane, Rockville, MD 20857, USA.

*To whom correspondence should be addressed.

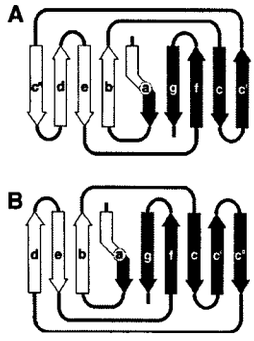

Fig. 2. Folding topology of (**A**) the V_α domain and (**B**) a typical V domain.

The CDR2 loops of V_α4.2 and V_β8.2 have the same conformation and superpose with an RMSD of 0.50 Å for six α carbon positions (Fig. 1B). The V_α CDR2 (Fig. 4B) appears to be stabilized by one intraloop backbone-backbone hydrogen bond (Arg^{51} O · · · N Glu^{54}) and by four additional backbone-backbone bonds with neighboring residues (Ala^{49} N · · · O Leu^{32}, Ala^{49} O · · · N Leu^{32}, Lys^{53} N · · · O Tyr^{65}, and Glu^{54} O · · · N Tyr^{65}). Four consecutive amino acids of CDR3 (Asn^{94}, Tyr^{95}, Gly^{96}, and Asn^{97}) had negligible electron density throughout the refinement. The atoms of these residues have been modeled in the structure, but because they were assigned zero occupancy, they were effectively excluded from the x-ray calculations. We conclude that CDR3 is disordered and that the two CDR3 loops in the homodimer are unable to pack together in a stable conformation. Such disorder may not be present in the intact αβ heterodimer. The loop comprising residues 67 to 72, which is analogous to the fourth hypervariable region of V_β (*3*), is one residue longer in V_α and folds away from CDR1. Because this loop forms part of a relatively flat continuous surface with the CDRs, it could potentially be involved in interactions with the peptide-MHC complex.

There is considerable evidence that TCRs must undergo dimerization (or oligomerization) for signal transduction to occur (*14*), as is the case for other cell-surface receptors (*15*). The structure and crystal packing of the V_α domain provide evidence that αβ TCRs can undergo dimerization, largely mediated through their α chains. Specifically, the β strand switch observed for V_α results in the removal of a surface

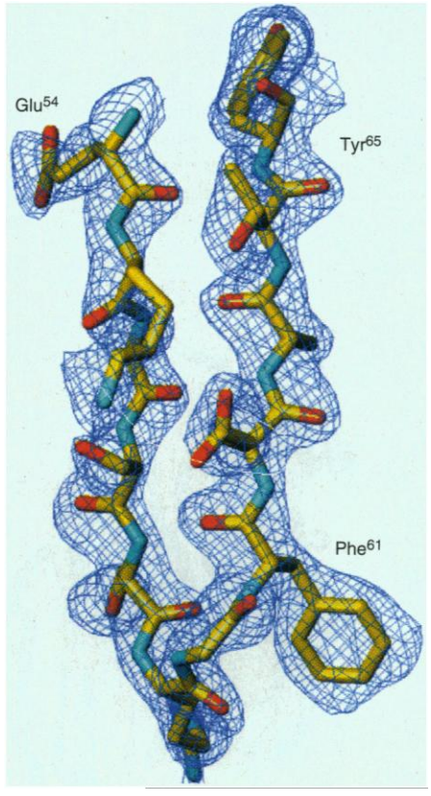

Fig. 3. $2F_o - F_c$ electron density map contoured at 1σ for the c′′ (left) and d (right) strands. Carbon, nitrogen, and oxygen atoms are colored yellow, blue, and red, respectively.

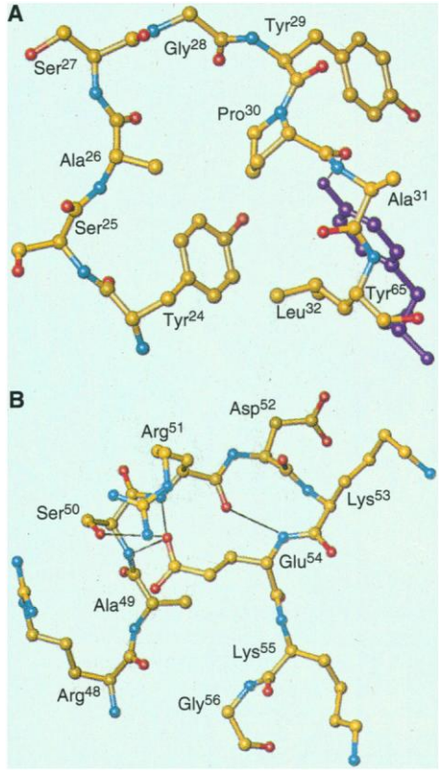

Fig. 4. V_α hypervariable loops. (**A**) CDR1; (**B**) CDR2. Hydrogen bonds are black lines; atoms are colored as in Fig. 3.

protrusion, which enables the homodimers to pack in a translational fashion along the crystallographic z axis, such that the peptide-MHC binding loops form a continuous patch on one face of the linear array (Fig. 5, A and B). Immunoglobulin V domains or V_β would be unable to pack in an analogous way because of steric hindrance. This raises the question of whether the TCR can dimerize in a way that is consistent with the V_α packing observed in this structure. A plausible model can indeed be constructed directly from the V_α crystal packing and the known structure of Vβ8.2, in which the V domains of a TCR $\alpha\beta$ heterodimer are packed as a tetramer and where most of the contacts in the $(V_\alpha V_\beta)_2$ dimer-dimer interface are formed between the two V_α domains (Fig. 5C).

Several observations suggest that the organization of V_α homodimers found in the crystal structure may represent a biologically relevant mode of association and is not simply a crystallization artifact. First, this particular packing arrangement is made possible by a unique strand switch not present in Ig V regions or in V_β. Second, a $(V_\alpha V_\beta)_2$ tetramer modeled on the basis of the observed mode of V_α association has all its CDR loops facing in one direction and disposed in essentially a single plane (Fig. 6), as might be expected for TCRs on a membrane surface. Third, the distribution of potential N-linked glycosylation sites on V_α and V_β domains is consistent with the idea that V_α-V_α interactions are functionally important. An examination of V_α and V_β sequences (*10*) reveals 14 and 12 such sites, respectively; their location in the crystal structures of V_α4.2 and Vβ8.2 is shown in Fig. 5C. None of these sites occurs in the putative interface between the two $V_\alpha V_\beta$ heterodimers in the tetramer model. Note that V_α domains lack N-linked glycosylation sites at positions corresponding to V_β residues 57, 60, 62, and 85. Glycosylation at the corresponding positions of V_α would be expected to interfere with tetramer formation (Fig. 5C).

If the parallel dimers observed in crystals of the V_α domain are assumed to reflect a physiological interaction, a mechanism that helps to explain signal transduction in T cells can be inferred. According to this mechanism, α chain–mediated TCR dimerization drives the formation of a homogeneous peptide–MHC class II dimer; binding of the class II dimer in turn stabilizes the weak TCR dimer sufficiently to result in receptor activation. In the absence of cognate peptide-MHC complexes, however, these putative TCR dimers exist only transiently on the cell surface, thus preventing T cells from triggering spontaneously. This cooperative mechanism, whereby weak TCR dimers interact with weak class II dimers to form stable TCR_2-MHC_2 signaling complexes, differs from that previously proposed (*16*, *17*) in that it assigns a central role to the TCR in driving the assembly of the signaling complex. Such a mechanism could explain how homogeneous peptide-MHC dimers can form on the surface of an antigen-presenting cell bearing hundreds of different peptide-MHC complexes.

Our model of a $(V_\alpha V_\beta)_2$ tetramer, based on the crystal packing of V_α homodimers, has obvious parallels to the human leukocyte antigen (HLA) class II dimer of dimers (*16*). In the orientation shown in Fig. 6A, the two sets of CDR3 loops (one set from each $\alpha\beta$ heterodimer) are well positioned to bind the two peptides in the crystal structure of the class II tetramer, such that V_α CDR3 would contact the NH_2-terminal portion of the peptide and V_β CDR3 would contact the COOH-terminal portion. The CDR1 and CDR2 loops of V_α would then interact primarily with the β1 domain of the class II molecule, and CDR1 and CDR2 of V_β would interact primarily with the α1 domain. This overall orientation best fulfills the criteria that V_α and V_β CDR3s interact mainly with bound peptide [as suggested by numerous mutagenesis and sequencing studies of TCRs of defined specificity (*2*)] and that, to the extent possible, each $\alpha\beta$ heterodimer in the TCR tetramer contacts only one class II molecule in the MHC tetramer. The positioning of V_α CDR3 over the NH_2-terminal portion of the antigenic peptide and of V_β CDR3 over the COOH-terminal residues in our structural model is in agreement with the orientation proposed by Jorgensen *et al.* (*18*) on the basis of amino acid changes in transgenic TCR α or β chains elicited by charge substitutions in the peptide.

An important difference in TCR-MHC tetramer-tetramer complementarity is also evident. Viewed from the side, the HLA class II dimer of dimers shows the two bound peptides at an angle of ~100° to each other, which precludes extensive interactions of both peptides with the relatively flat surface of the putative TCR tetramer (Fig. 6B). A conformational change in the MHC class II dimer of dimers or the TCR dimer of dimers, or both, would be necessary to achieve a TCR-MHC tetramer-tetramer interface in which most or all of the residues in the two peptides are in contact with the TCR. With respect to possible conformational changes in the HLA-DR1 dimer of dimers, Goodman *et al.* (*19*) tested the effects on T cell activation of mutations at residues Glu^{88} and Lys^{111} of the DRα chain, which form two reciprocal salt bridges in the crystal structure (*16*). Although substitu-

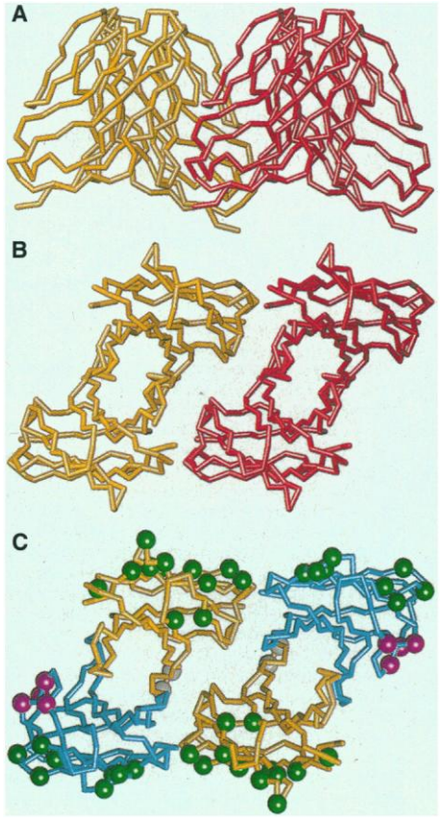

Fig. 5. V_α tetramer and model of a $(V_\alpha V_\beta)_2$ tetramer. (**A**) Packing of two V_α dimers as observed in the crystal structure, with the CDR loops at the top of the aggregate. The packing arises from a crystallographic translation of homodimers along the z axis (horizontal here). (**B**) View of two V_α dimers looking down on the CDR loops. (**C**) Model of a $(V_\alpha V_\beta)_2$ tetramer oriented as in (B), with potential N-linked glycosylation sites shown as spheres. V_α and V_β are colored yellow and blue, respectively. The model of the 1934.4 V_β domain was made by replacing CDR3 of the known structure of the 14.3.d V_β domain (*3*) with the backbone of the V_L CDR3 loop of the catalytic antibody 17E8 (PDB accession number 1EAP) (*23*); this CDR3 loop has the same length as that of the 1934.4 V_β domain. The 1934.4 and 14.3.d TCRs use the same V_β gene segment (Vβ8.2) and closely related J_β segments. Amino acid substitutions in CDR3 and subsequent energy minimization resulted in a plausible model for the 1934.4 V_β domain. The $V_\alpha V_\beta$ heterodimer was constructed by superposing the V_β model onto a V_α domain of the V_α homodimer. The heterodimer-heterodimer interface in the tetramer is made of contacts predominantly between the V_α domains in the vicinity of the c′′ strand switch. Higher degrees of translational aggregation would be prevented by steric hindrance between V_β domains arising from the position of the V_β c′′ strand. The N-linked glycosylation sites at V_β positions 57, 60, 62, and 85 are colored purple; analogous sites are absent in V_α chains. Two glycosylation sites at the base of the $(V_\alpha V_\beta)_2$ tetramer that are not implicated in the heterodimer-heterodimer interface are shown in gray.

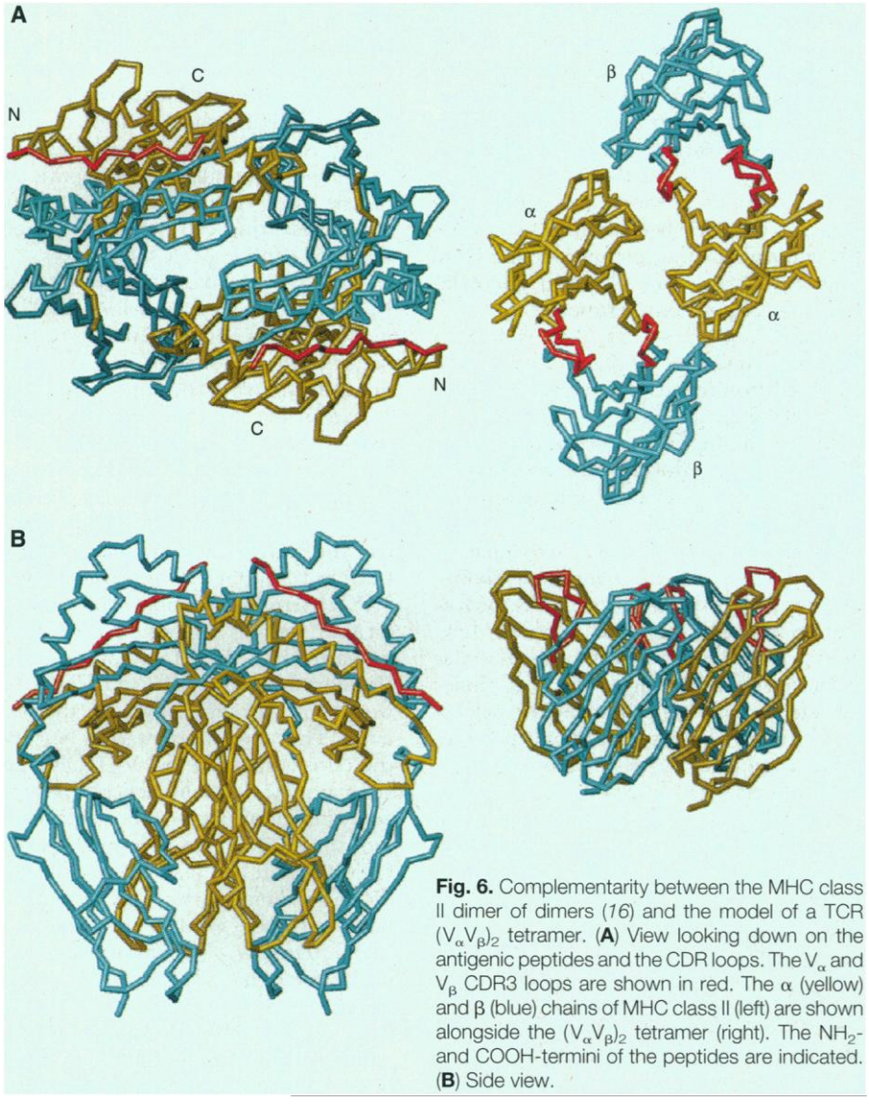

Fig. 6. Complementarity between the MHC class II dimer of dimers (*16*) and the model of a TCR $(V_\alpha V_\beta)_2$ tetramer. (**A**) View looking down on the antigenic peptides and the CDR loops. The V_α and V_β CDR3 loops are shown in red. The α (yellow) and β (blue) chains of MHC class II (left) are shown alongside the $(V_\alpha V_\beta)_2$ tetramer (right). The NH_2- and COOH-termini of the peptides are indicated. (**B**) Side view.

tions at position 88 were found to abolish antigen presentation, mutations at position 111 had no obvious effect. One interpretation of these results is that although the interaction between DRα residues 88 and 111 is present in the crystal structure of the unliganded HLA-DR1 tetramer, this interaction is not preserved in the putative TCR_2-MHC_2 complex because of a rearrangement in the MHC dimer-dimer interface upon TCR binding. Thus, T cell signaling may involve conformational changes in the TCR or MHC moieties, or both, associated with receptor dimerization.

REFERENCES AND NOTES

1. M. Kronenberg *et al.*, *Annu. Rev. Immunol.* **4**, 529 (1986); S. Porcelli *et al.*, *Immunol. Rev.* **120**, 137 (1991).
2. J. B. Rothbard and M. L. Gefter, *Annu. Rev. Immunol.* **9**, 527 (1991); J. L. Jorgensen *et al.*, *ibid.* **10**, 835 (1992).
3. G. A. Bentley *et al.*, *Science* **267**, 1984 (1995).
4. S. S. Zamvil *et al.*, *Nature* **324**, 258 (1986).
5. H. Acha-Orbea *et al.*, *Cell* **54**, 263 (1988).
6. S. Zamvil *et al.*, *Nature* **317**, 355 (1985); L. Steinman, *Adv. Immunol.* **49**, 357 (1991).
7. E. S. Ward, *J. Mol. Biol.* **224**, 885 (1992).
8. B. A. Fields *et al.*, *ibid.* **239**, 339 (1994).
9. Orthorhombic crystals, space group $P2_12_12$, were grown in 1.9 M Li_2SO_4-at pH 8, as described (*8*). Unit cell dimensions were a = 97.7 Å, b = 79.6 Å, and c = 30.5 Å, with one V_α homodimer in the asymmetric unit. A total of five crystals were used for x-ray data collection at room temperature. Data from three crystals were collected on a Siemens area detector and processed with the program XENGEN (*20*); the resulting 71,748 observations to 2.04 Å resolution were merged to give 14,353 unique reflections (R_{merge} = 0.125, where $R_{merge} = \Sigma|I - \langle I\rangle|/\Sigma\langle I\rangle$ and I is the reflection intensity). Values of R_{merge} for the individual data sets were 0.067, 0.084, and 0.097. Data from two crystals were collected on a MAR image plate instrument; the resulting 50,330 observations to 1.90 Å resolution were merged to give 15,428 unique reflections (R_{merge} = 0.120). Individual R_{merge} values were 0.080 and 0.102. The Siemens and MAR data sets were merged without rejection to give 16,604 unique reflections (R_{merge} = 0.144), with structure factor amplitude $F > 0$, to 1.9 Å resolution. Data completeness is 95.6% in the range 10.0 to 2.2 Å and 88.2% in the range 2.3 to 2.2 Å. The structure was solved by the molecular replacement method with the use of the program AMoRe (*21*). The search model comprised the N, C, O, Cα, and Cβ atoms of both chains of the Bence-Jones dimer REI [Brookhaven Protein Data Bank (PDB) accession number 1REI] [O. Epp *et al.*, *Eur. J. Biochem.* **45**, 513 (1974); O. Epp *et al.*, *Biochemistry* **14**, 4943 (1975)]. The translation-function peak with the highest correlation coefficient corresponded to the 17th highest peak in the cross-rotation function. Rigid body refinement of this solution with 8 to 4 Å data resulted in a reduction of R from 0.542 to 0.525 (where $R = \Sigma|F_o - F_c|/\Sigma F_c$, F_o is the observed F, and F_c is the calculated F) and an increase of 22.6% in the correlation coefficient. Several other potential solutions did not show such favorable behavior. The solution made packing sense and was also consistent with the presence of a large self-Patterson peak at (0.50, 0.47, 0.00). The noncrystallographic twofold axis relating the two monomers in the dimer is almost coincident with the crystallographic a axis, and this combination of crystallographic and noncrystallographic symmetry can be shown algebraically to give rise to the self-Patterson peak near (0.5, 0.5, 0.0). Refinement with X-PLOR (*22*) and the merged Siemens data gave R_{work} (the R for reflections used in the refinement) = 0.200 for 6.0 to 2.3 Å data (8054 reflections) and R_{free} (the R for 10% of the reflections in the data set excluded from refinement) = 0.287 for the 782 reflections excluded from the refinement until the final cycles. At this stage the MAR data became available, and although they were of only slightly higher effective resolution, they did prove useful for cross validation, thus enabling an independent calculation of R_{free}. The R factor (R_{free}) calculated with the Siemens refined coordinates and the new MAR data was 0.238 for 6.0 to 2.2 Å data with $F > 2\sigma F$. Inclusion of data beyond 2.2 Å resolution did not result in improved maps or enable the location of additional solvent sites, presumably because of the weakness of these data. The final R for the structure refined against the merged Siemens and MAR data is 0.205 for the 9682 reflections with $F > 2\sigma F$ in the range 6.0 to 2.2 Å. Data completeness corresponding to these reflections is 80.7% for the range 6.0 to 2.2 Å and 57.5% for the 2.3 to 2.2 Å shell. RMSDs of the geometry parameters from standard values are 0.012 Å for bond lengths and 2.02° for bond angles. The model includes 40 water molecules. A Ramachandran plot shows that no residues lie in disallowed regions.
10. E. A. Kabat *et al.*, *Sequences of Proteins of Immunological Interest* (Public Health Service, NIH, Washington, DC, ed. 5, 1991).
11. L. M. Amzel and R. J. Poljak, *Annu. Rev. Biochem.* **48**, 961 (1979).
12. C. Chothia *et al.*, *J. Mol. Biol.* **186**, 651 (1985).
13. P. Bork, L. Holm, C. Sander, *ibid.* **242**, 309 (1994); Y. Harpaz and C. Chothia, *ibid.* **238**, 528 (1994).
14. J. Kaye *et al.*, *J. Exp. Med.* **158**, 836 (1983); J. Kappler *et al.*, *Cell* **34**, 727 (1983); S. C. Meuer *et al.*, *J. Exp. Med.* **158**, 988 (1983); J.-P. Abastado *et al.*, *ibid.* **182**, 439 (1995).
15. A. Ullrich and J. Schlessinger, *Cell* **61**, 203 (1990); C.-H. Heldin, *ibid.* **80**, 213 (1995); W. Kolanus, C. Romeo, B. Seed, *ibid.* **74**, 171 (1993); A. Weiss and D. Littman, *ibid.* **76**, 263 (1994).
16. J. H. Brown *et al.*, *Nature* **364**, 33 (1993).
17. R. N. Germain, *Curr. Biol.* **3**, 586 (1993); *Cell* **76**, 287 (1994).
18. J. L. Jorgensen *et al.*, *Nature* **355**, 224 (1992).
19. S. Goodman *et al.*, *J. Immunol.* **155**, 1210 (1995).
20. A. J. Howard *et al.*, *J. Appl. Crystallogr.* **20**, 383 (1987).
21. J. Navaza, *Acta Crystallogr.* **A50**, 157 (1994).
22. A. T. Brünger, *X-PLOR Version 3.1* (Yale Univ. Press, New Haven, 1992).
23. G. W. Zhou *et al.*, *Science* **265**, 1059 (1994).

24. We thank R. J. Poljak, K. Karjalainen, J. T. Pedersen, A. M. Silva, P. Collins, and D. Wraith for discussions and advice. Supported by NIH grants GM52801 (R.A.M.) and AI31592 (E.S.W.), National Multiple Sclerosis Society grants RG 2747 (R.A.M.) and 2411 (E.S.W.), the Richard Lounsbery Foundation (R.A.M.), the Yellow Rose Gala (E.S.W.), and CONICET, Argentina (E.L.M.).

23 August 1995; accepted 27 October 1995